AIP | The Journal of Chemical Physics

Direct observation of surface reactions by scanning tunneling microscopy: Ethylene→ethylidyne→carbon particles→graphite on Pt(111)

T. A. Land, T. Michely, R. J. Behm, J. C. Hemminger, and G. Comsa

Citation: J. Chem. Phys. **97**, 6774 (1992); doi: 10.1063/1.463655
View online: http://dx.doi.org/10.1063/1.463655
View Table of Contents: http://jcp.aip.org/resource/1/JCPSA6/v97/i9
Published by the AIP Publishing LLC.

Direct observation of surface reactions by scanning tunneling microscopy: Ethylene→ethylidyne→carbon particles→graphite on Pt(111)

T. A. Land
IGV, Forschungszentrum (KFA) Jülich, Postfach 1913, W 5170 Jülich, Germany and Department of Chemistry and Institute for Surface and Interface Science, University of California, Irvine, California 92717

T. Michely
IGV, Forschungszentrum (KFA) Jülich, Postfach 1913, W 5170 Jülich, Germany

R. J. Behm
Department of Surface Chemistry and Catalysis, University Ulm, Postfach 4066, D W 7900 Ulm, Germany

J. C. Hemminger
Department of Chemistry and Institute for Surface and Interface Science, University of California, Irvine, California 92717

G. Comsa
IGV, Forschungszentrum (KFA) Jülich, Postfach 1913, W 5170 Jülich, Germany

(Received 14 May 1992; accepted 6 July 1992)

We have used variable temperature, ultrahigh vacuum scanning tunneling microscopy (STM), in both static and time-dependent experiments, to study the chemistry of the ethylene/Pt(111) system. Images of ethylene which exhibit long-range order have been obtained at a sample temperature of 160 K. The conversion of ethylene to ethylidyne has been observed directly in STM images. This conversion reaction is observed to occur in a "patchy" manner across the surface at saturation coverage. As the reaction proceeds, well-defined islands of unreacted ethylene continue to be clearly observed. Further dehydrogenation of the ethylidyne formed from ethylene leads to carbon containing particles dispersed randomly across the sample. After annealing the ethylidyne covered sample to 500 K, the surface is uniformly covered with carbon containing particles which exhibit a bimodal distribution of heights (one and two atomic layers) consisting of an average of ten and twenty carbon atoms, respectively. Further annealing to 700 K results in the formation of larger particles which appear to be a single atomic layer high and 10–15 Å in diameter in the STM images. These particles contain an average of thirty-four carbon atoms. Pt steps do not show any preferential reactivity for these reactions. Annealing the carbon particle covered surface to higher temperatures results in the formation of monolayer thick graphite islands, which eventually accumulate at the Pt steps.

INTRODUCTION

Adsorbed ethylene has often been used as a model for hydrogenation–dehydrogenation reactions in catalysis studies.[1,2] In particular, the interaction of ethylene with the close-packed Pt(111) surface has been investigated by a wide variety of surface science techniques.[3–30] These studies have focused on many aspects such as the identity of the molecular adsorbates as a function of temperature, kinetics of the reactions, and catalytic reactivity of the system. Figure 1 reviews some of the structural aspects of the adsorption and decomposition of ethylene. It is known that ethylene adsorbs intact with the C=C bond axis parallel to the Pt(111) surface at temperatures up to 200 K.[6,10,12] At surface temperatures above 230 K, ethylene (C_2H_4) converts irreversibly to ethylidyne (CCH_3) by loss of hydrogen. The C–C bond axis of ethylidyne is perpendicular to the surface.[6,9–12,16,26] The kinetics of this reaction at saturation monolayer coverage have been investigated by several methods and have been shown to follow first-order kinetics with respect to ethylene coverage.[5,7,23,27] Surface hydrogen generated in the formation of ethylidyne desorbs from the Pt surface at ~350 K leaving ethylidyne as the only stable molecular species on the surface at this temperature.[6,7,9–11,16,26] The ethylidyne species is stable on the Pt(111) surface at temperatures up to 430 K. An ordered (2×2) low-energy electron diffraction (LEED) pattern is reported for the room temperature ethylidyne phase.[10,11,26] However, the actual molecular arrangement and coverage remains controversial with the LEED (2×2) pattern interpreted as a (2×2) structure with an ideal coverage of 0.25 ML of ethylidyne (ML—here one monolayer is taken as a coverage of one molecule per surface Pt atom),[9,11,19,26,30] or in terms of higher coverage structures, e.g., three domains of a (2×1) structure[14] or a honeycomb structure[15,28] with a coverage of 0.50 ML of ethylidyne. The LEED pattern observed for ethylene at low temperature is more complicated and has been reported by some researchers as a disordered structure.[26] Others report a series of several LEED patterns for the ethylene/ethylidyne on the Pt(111) system occurring over the temperature range of 100–300 K.[10] Details of the highly ordered structure which we observe by STM will be presented in Ref. 29.

 0021-9606/92/216774-10$006.00

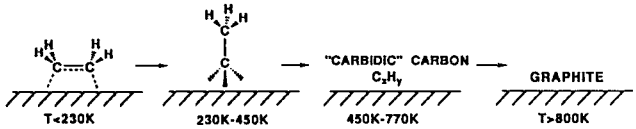

FIG. 1. A schematic review of what was previously known about the adsorption and decomposition of ethylene on Pt(111).

Heating the Pt sample above 450 K results in dehydrogenation of the ethylidyne and finally at 700 K all of the hydrogen has been removed from the surface and only carbon remains.[7,11,13,18] The carbonaceous species formed from the decomposition of ethylidyne and other hydrocarbons on Pt in the temperature range 450–700 K is not graphitic in nature and has been labeled as "carbidic" carbon in the literature.[1,2,7,13,18,20] The intermediate decomposition products are of interest in catalysis as it is the carbidic carbon that appears to play an active role in catalytic processes and graphitic carbon that acts as a poison to catalytic activity.[1,2]

It has previously been proposed that surface defects such as steps and kinks catalyze adsorption and dissociation reactions associated with heterogeneous catalysis reactions.[21,22,25,31] This was concluded from results of systematic case studies on surfaces with varying step densities.[32] The actual role and activity of defect sites in catalytic reactions, however, is still under debate. Clearly this will sensitively depend on the specific reaction. Local probe studies such as those described here can provide direct information on this topic.

LEED experiments have been used to detect graphite formation on the Pt surface.[33,34] A characteristic graphite ring diffraction pattern is observed in LEED experiments following annealing of carbon covered Pt surfaces to $T \sim 800$ K. After annealing to higher temperatures, some segmentation of the ring diffraction pattern is observed indicating that there is a preferential alignment of the graphite with the Pt substrate. STM experiments have provided detailed information on the alignment and nature of the graphite layer.[4] LEED studies have led to the development of several models for graphite formation on Pt. Models based on both limited multilayer formation[33] and growth of the graphite layer on top of an intercalated layer of carbidic carbon have been proposed.[34] Our STM experiments have shown that decomposition of a hydrocarbon monolayer results in the formation of monolayer high islands of graphite on the Pt surface, i.e., a single layer of carbon atoms in a graphitic arrangement (graphene layer) rests on the Pt(111) substrate.[4]

We report here on STM experiments which result in a substantially new understanding of the chemistry of ethylene, ethylidyne, and carbidic carbon on Pt(111). We have been able to resolve ethylene molecules in STM images recorded at 160 K, anneal the sample at controlled temperatures to 230 K, and observe the conversion of ethylene to ethylidyne. Images recorded *in situ* during decomposition of ethylene into ethylidyne revealed that the reaction occurs preferentially at the perimeter of islands of unreacted ethylene. Our experiments also show that further decomposition of ethylidyne with annealing above 450 K proceeds through a series of carbonaceous particle intermediates to eventually form graphite at temperatures above 800 K. STM images obtained after annealing in the range 430–700 K show no special reactivity of the Pt step edges in the decomposition of either ethylene, or ethylidyne.

EXPERIMENTAL

Experiments were performed at the IGV/KFA in Jülich, Germany with a specially designed microscope which is based on the "beetle" type STM.[35,36] The microscope is incorporated in an ultrahigh vacuum (UHV) system with standard techniques for sample preparation and characterization such as LEED and Auger electron spectroscopy. The Pt(111) crystal is mounted in a fixed, ramped sample holder. The sample assembly is mounted on a thermally insulated copper block which is damped against vibrations and contained in a rigid manipulator tube with two degrees of freedom, rotation, and translation for easy sample positioning. The sample can be heated from the back by means of a hot filament and the entire sample assembly is in contact with a liquid nitrogen reservoir which can be used to cool the sample to 150 K. Sample temperature control is possible in all preparation and analysis steps. STM measurements can be performed over a wide, controlled temperature range from 150 to 450 K. Experiments which involve sample temperatures above 450 K require that the STM be lifted from the sample. This is accomplished in a quite facile manner and images can be obtained within 10 min of a flash anneal to as high as 1200 K. Annealing experiments discussed in this paper were accomplished by quickly flashing the sample to the desired temperature and holding the sample at that temperature for 5 s, if not otherwise indicated. All images were obtained in the constant current mode with tunneling currents of 1.5 to 15 nA, and typical bias voltages of ± 30 to ± 200 mV applied to the tip. A scan frequency of 8 Hz was typically used to obtain topographs of 512×512 lines. The high quality Pt(111) sample is very well oriented and polished and exhibits an average terrace width of 2000 Å.[37] The orientation of the Pt crystal in our STM images has been inferred from x-ray diffraction measurements.[38] Sample cleaning was accomplished by standard procedures of oxygen treatment and argon ion bombardment, and checked with Auger electron spectroscopy. The clean surface was then exposed to varying amounts of ethylene by backfilling the chamber. Exposures of 2.5 L (1 L $= 1 \times 10^{-6}$ Torr s) resulted in a saturation coverage of ethylene at 160 K. Room temperature exposures were typically over 5 L to ensure saturation.

RESULTS AND DISCUSSION

The adsorption and reactions of ethylene adsorbed in UHV on Pt(111) have been studied as a function of temperature by STM. STM images recorded on a Pt(111) surface after a saturation exposure of ethylene at 160 K, with the sample held at this temperature, reveal a regular

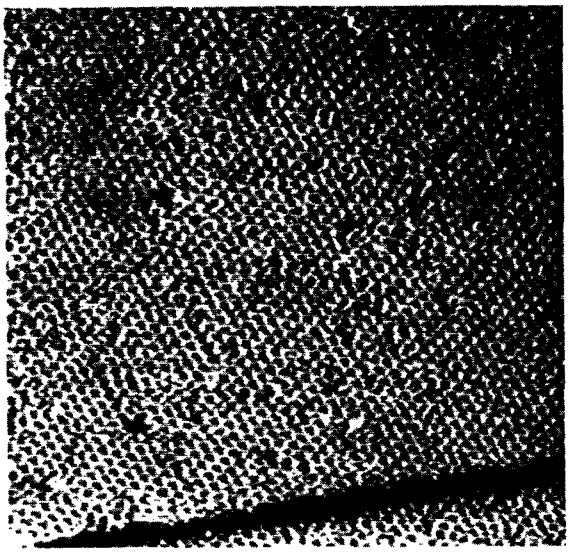

FIG. 2. This 400 Å×400 Å image was obtained at 160 K after adsorption of ethylene at this temperature. On this scale, one does not resolve the individual molecules, but rather one observes the overall pattern that is formed by the molecular arrangement. The feature in the lower part of the image is a Pt step edge.

pattern formed by the ethylene molecules as seen in Fig. 2. In this 400 Å×400 Å image, one can see that the regular pattern extends over quite large distances. The structural aspects of this system will be discussed in detail in a future publication.[29]

After annealing the sample to 350 K, ethylidyne is the only stable surface species.[6,7,9–11,16,26] In STM images taken after annealing the ethylene overlayer to 300–350 K, or upon exposure of the crystal to ethylene at these temperatures, no discernible structure is resolved (STM images were taken at room temperature or at the annealing temperature). It is interesting that no structure is observed by STM even though ethylidyne is present and, as we verified by LEED experiments in our laboratory, exhibits an ordered (2×2) LEED pattern that is stable until 430 K. Only cooling of an ethylidyne covered surface does allow us to resolve this intermediate. Figure 3(a) and 3(b) show 200 Å×200 Å and 400 Å×400 Å images obtained at 180 and 230 K, respectively, after forming ethylidyne at 350 K. The origin of this apparent contradiction (probably due to low frequency vibrations which blur the corrugation in STM images of the close packed ethylidyne at higher temperatures) will be discussed together with structural aspects of this adlayer in a forthcoming publication.[29]

Since, as can be seen from Figs. 2 and 3, we can resolve and distinguish ethylene (long-range order and sharper pattern) and ethylidyne (rather disordered and fuzzier pattern) under reaction conditions, we are now in a position to use STM to follow the conversion reaction. Previous kinetics experiments have shown that the conversion from ethylene to ethylidyne begins at 230 K and is nearly complete after ~10 min at this temperature.[7] These experiments have also shown that this reaction follows a rate law

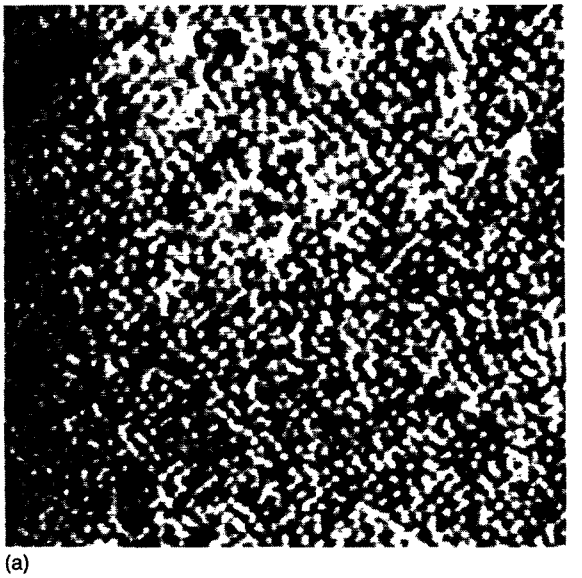

(a)

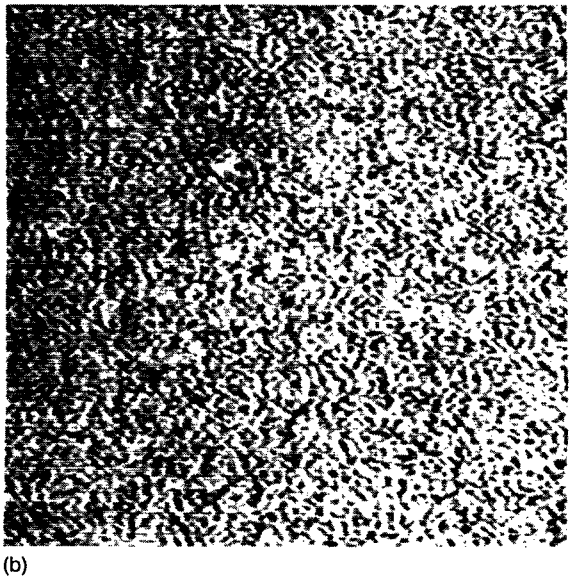

(b)

FIG. 3. (a) This 200 Å×200 Å image was obtained at 180 K after annealing the ethylene overlayer to 350 K to form ethylidyne and recooling the sample to 180 K. The individual dots seen in the image correspond to the ethylidyne molecules. (b) This 400 Å×400 Å image was obtained at 230 K after annealing the ethylene overlayer at 230 K for ~15 min resulting in complete conversion to ethylidyne.

which is first order in ethylene coverage.[5,7,23,27] *In situ* STM imaging allows us to directly follow the spatial development of the decomposition process, converting adsorbed ethylene into adsorbed ethylidyne. This is demonstrated in the two 400 Å×400 Å STM images in Fig. 4, which were recorded during the reaction process at 230 K. The image in Fig. 4(a), was obtained after holding the sample for several minutes at this temperature, corresponding to a partially reacted surface. The second image in Fig. 4(b) was recorded on practically the same area of the surface, but several minutes later. This is demonstrated by the two white protrusions in the lower half of Fig. 4(a), which are only slightly shifted lower in the image in Fig.

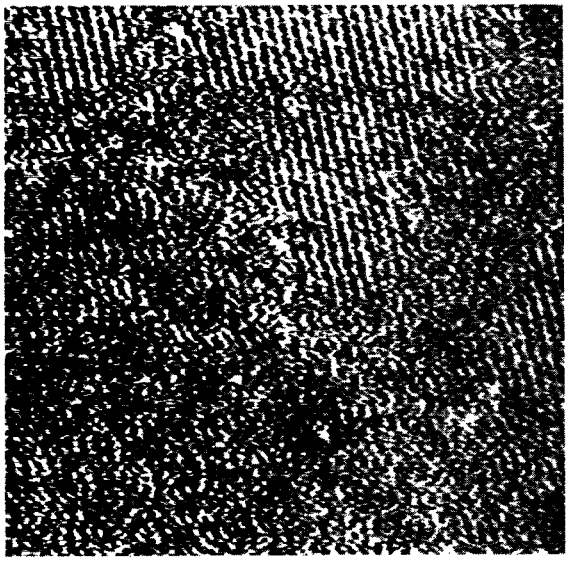

(a)

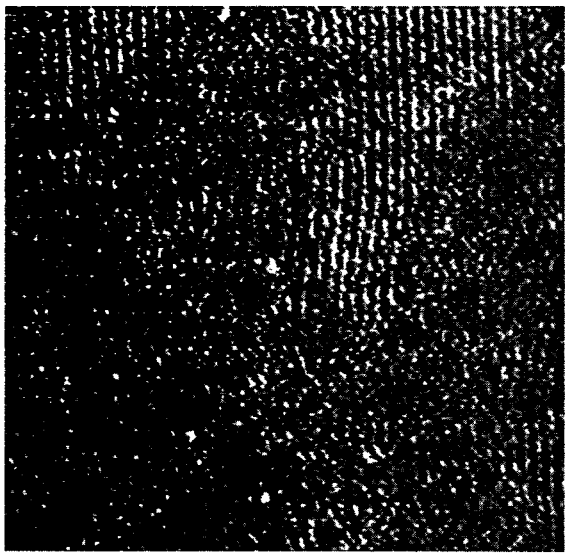

(b)

FIG. 4. These 400 Å×400 Å images were obtained as a function of time at 230 K. In these images, areas covered by ethylene molecules appear as the well-ordered pattern, and areas covered by ethylidyne molecules appear as a rather disordered pattern. (a) This image was obtained after annealing the sample for several minutes at 230 K. (b) This image was obtained on the same area of the surface kept for several additional minutes at the same temperature after the image shown in (a).

4(b). In these images, ethylene, which lies parallel to the surface, appears as a well-ordered sharper structure as seen in the top center, upper left, and middle right edge of the image in Fig. 4(a). Ethylidyne, which is perpendicular to the surface appears as the somewhat fuzzy less-ordered structure seen in the rest of the image [see Figs. 2 and 3(b) for comparison]. Clearly the reaction does not proceed randomly over the surface, as one would expect from a straightforward interpretation of a simple model of first-order kinetics. Instead, by comparing the two images, it appears that the reaction takes place at the edges of ethylene islands. While there are various mechanisms by which the observed behavior can be consistent with the observation of first-order kinetics, it is not expected for the simple random reaction probability concept normally associated with a first-order process.

Heating of ethylidyne covered Pt(111) to temperatures above 430 K results in further dehydrogenation. As is known from thermal desorption spectroscopy (TDS) and high-resolution electron-energy-loss spectroscopy (HREELS) experiments, heating the sample to 700 K leads to complete dehydrogenation, leaving carbon on the surface (see Fig. 1).[7,11,13,18] From LEED measurements, we know, however, that graphite is not formed unless the sample is heated to temperatures above 800 K. The set of STM images in Fig. 5, which were taken at room temperature after annealing, show changes in the morphology of the adlayer following annealing to temperatures in the range 430–700 K. In contrast to the images of the ethylidyne layer taken at room temperature where no structure is resolved with the STM, one observes a few small protrusions appearing in the image after annealing the sample to 430 K as seen in Fig. 5(a). The rest of the image area is still covered with nondehydrogenated ethylidyne. Following annealing of the sample to 450 [Fig. 5(b)] and 500 K [Fig. 5(c)], one sees an increase in the number of protrusions with a maximum density of protrusions appearing near 500 K. We associate these protrusions with carbonaceous particles resulting from dehydrogenation reactions. Indeed, the first appearance of these particles corresponds to the onset of hydrogen desorption from ethylidyne dehydrogenation as seen in TDS experiments.[11,13,18] In contrast to ethylidyne which is only visible to the STM with the sample at low temperature, the carbonaceous particles seen in Fig. 5 are well resolved in the images taken at room temperature. This is true even for low initial exposures of ethylene (0.15 L) suggesting that the particles are immobile. This is in contrast to the behavior which we observe for intact, molecularly adsorbed ethylene, even at 160 K, and for naphthalene and azulene at room temperature on Pt(111). High quality images of these molecular adsorbates are obtained only at near saturation coverages. At lower coverages, these molecules are sufficiently mobile on the flat Pt(111) surface that images cannot be obtained due to either thermally induced or tip-induced diffusion.

TDS experiments show that when the sample is annealed to 700 K, all the hydrogen is removed and only carbon remains on the surface.[7,11,13,18] As seen in Fig. 6, which was obtained at room temperature after annealing the sample to 700 K, the carbonaceous particles have become larger and exhibit a more uniform size. Similar images are also seen after annealing the sample to 770 K. In the 1000 Å×1000 Å image in Fig. 6(a), one observes that the carbonaceous particles are rather uniform in appearance and are more or less evenly distributed over the surface. In particular, there is no aggregation of the particles at step edges. In the 200 Å×200 Å image shown in Fig. 6(b), one observes the appearance of well-resolved particles of 10–15 Å diameter. In the images shown in Fig. 6, one sees some areas where the particles appear to line up forming elongated clusters. Even the areas which appear as

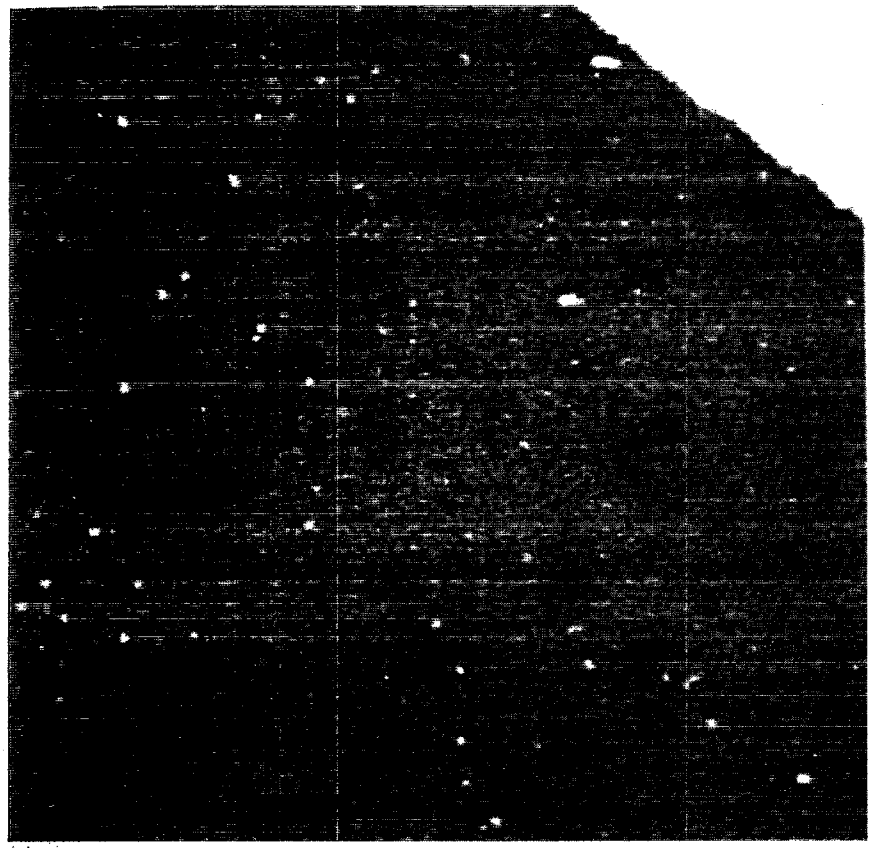

(a)

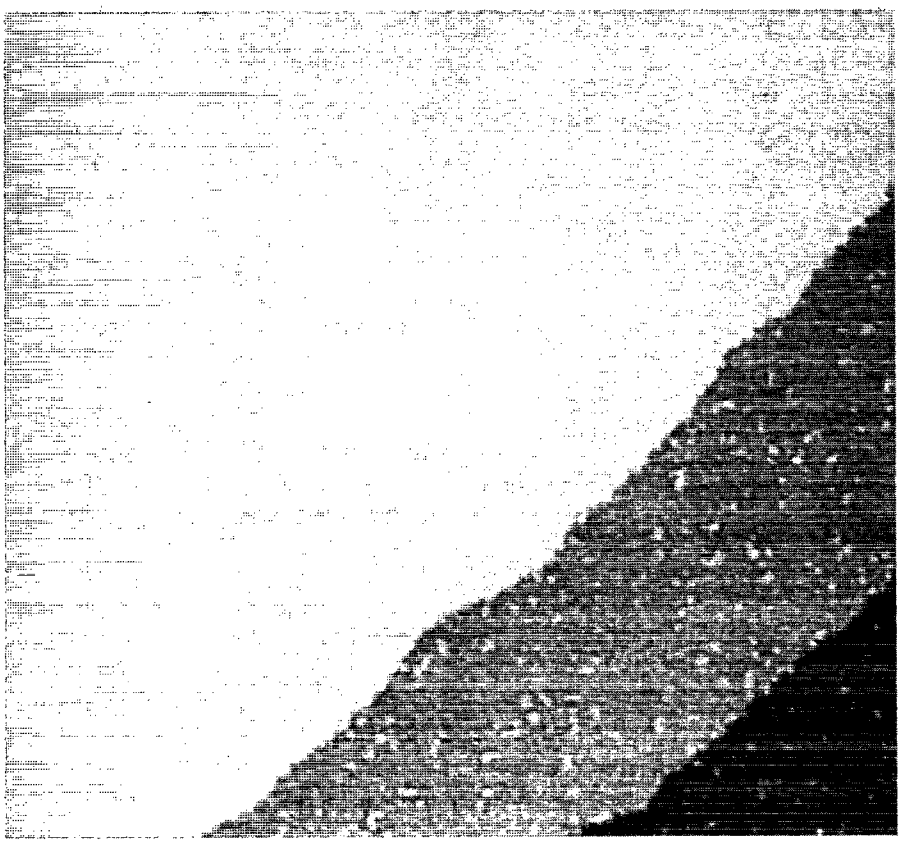

(b)

FIG. 5. This set of 1000 Å×1000 Å images were obtained at room temperature after annealing the sample for 5 s to the indicated temperature (a) 430; (b) 450; and (c) 500 K. The protrusions appearing in the images correspond to carbonaceous particles resulting from further dehydrogenation of ethylidyne with annealing of the sample.

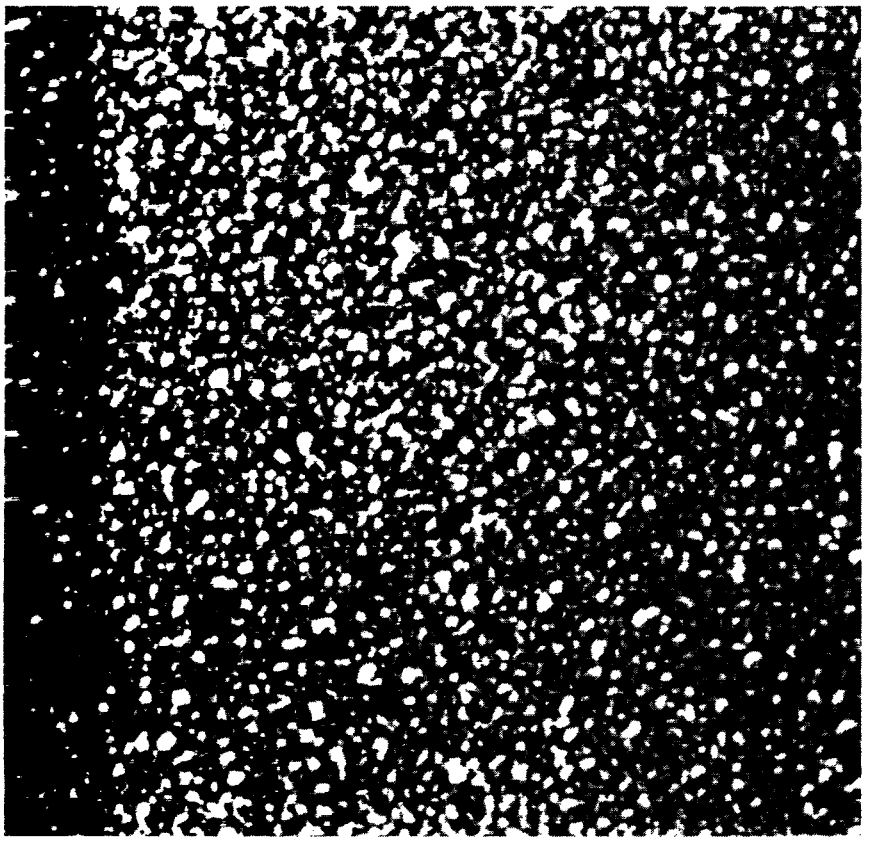

(c)

Fig. 5 (*Continued*).

clusters are clearly seen to actually be composed of these smaller particles. It is interesting to note that round clusters of particles are not observed. It is important to recognize that the detailed topography of a STM image is a convolution of sample and tip effects and is especially subject to electronic structure effects. The apparent sizes of the particles described here may be affected by such phenomena. The in-plane dimensions of the particles were observed to be similar in different experiments involving a number of different tips, indicating that they depend little on tip size effects. One should note that the individual particles which are 10–15 Å in diameter are much larger than those expected for individual carbon atoms or even small carbon clusters. In the past, it has been suggested that hydrocarbon decomposition proceeded to individual carbon atoms (Ref. 13 and references in Ref. 17). In recent secondary ion mass spectroscopy (SIMS)[18] experiments, in addition to individual carbon atoms, larger C_x fragments, where $x=2$ or 3, have been observed. These results along with Auger[20] experiments indicate maintenance of the C–C bonds above the temperature of the initial dehydrogenation of ethylidyne. The bulk of the previous literature which discusses the carbonaceous species in this temperature range, referred to carbidic carbon which was generally thought of as individual carbon atoms adsorbed on the surface.

A better way to determine the actual size of the adparticles, i.e., the average number of carbon atoms per particle, is based on a density evaluation. We can estimate the number of carbon atoms in each particle since we know the starting ethylidyne coverage to be ~ 0.20 ML of molecules,[29] and we know that no carbon containing species desorb from the surface during ethylidyne dehydrogenation. Also, carbon dissolution into the bulk is not important for the temperatures discussed here and is very low in any case as Pt forms no interstitial carbides.[39] If we assume that after annealing to 700 K all surface carbon has been converted into adparticles visible in these images, we can simply count the number of particles in an imaged area and use the known carbon coverage to obtain an average number of carbon atoms per particle. This analysis leads to an average of $\sim 34 \pm 7$ carbon atoms per particle after annealing the sample to 700 K. Clearly, the existence of such large carbonaceous particles indicates that new C–C bonds are being formed as the ethylidyne is dehydrogenated. The particle size following annealing to 700 K is sufficiently large to accommodate the 34 carbon atoms in a single layer.

A more detailed analysis of the particle heights reveals interesting differences between the particles formed at 500 K and those formed at 773 K, where the latter ones are essentially identical to those formed at 700 K, which we have just described. Figure 7 shows experimental particle height distributions obtained from images following annealing of the sample to 500 [Fig. 7(a)] and 773 K [Fig. 7(b)]. The experimental distributions were obtained by tabulating the heights of a large number of particles from each image (772 particles for the 500 K image and 295 particles for the 773 K image). The plots shown in Fig. 7 contain data from one 773 K image and one 500 K image,

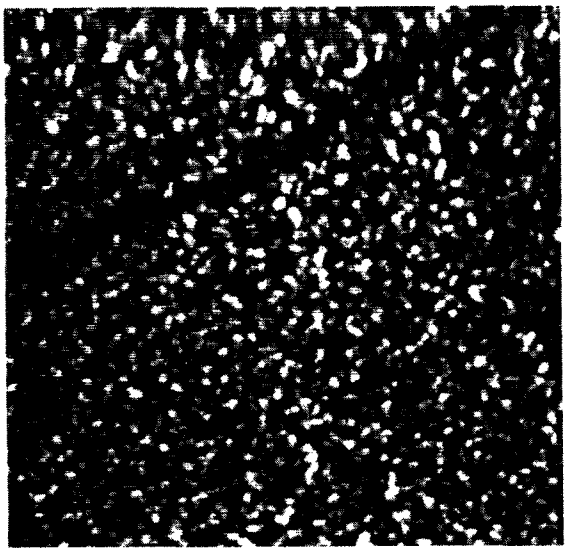

(a)

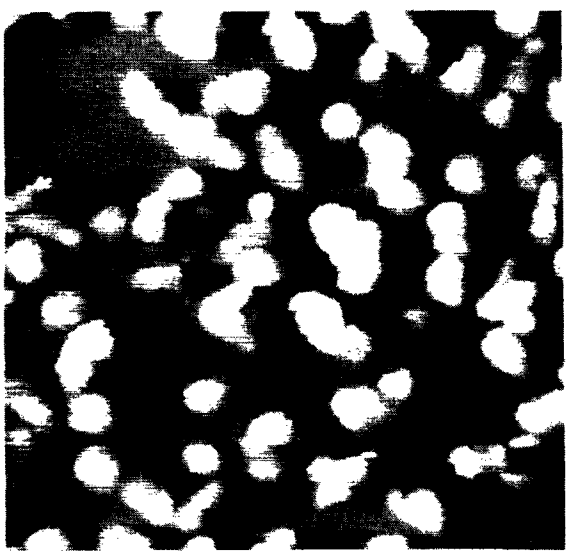

(b)

FIG. 6. These two images were obtained at room temperature showing the carbon particles which result from annealing the sample to 700 K for 5 s. (a) A 1000 Å×1000 Å image and (b) a 200 Å×200 Å image.

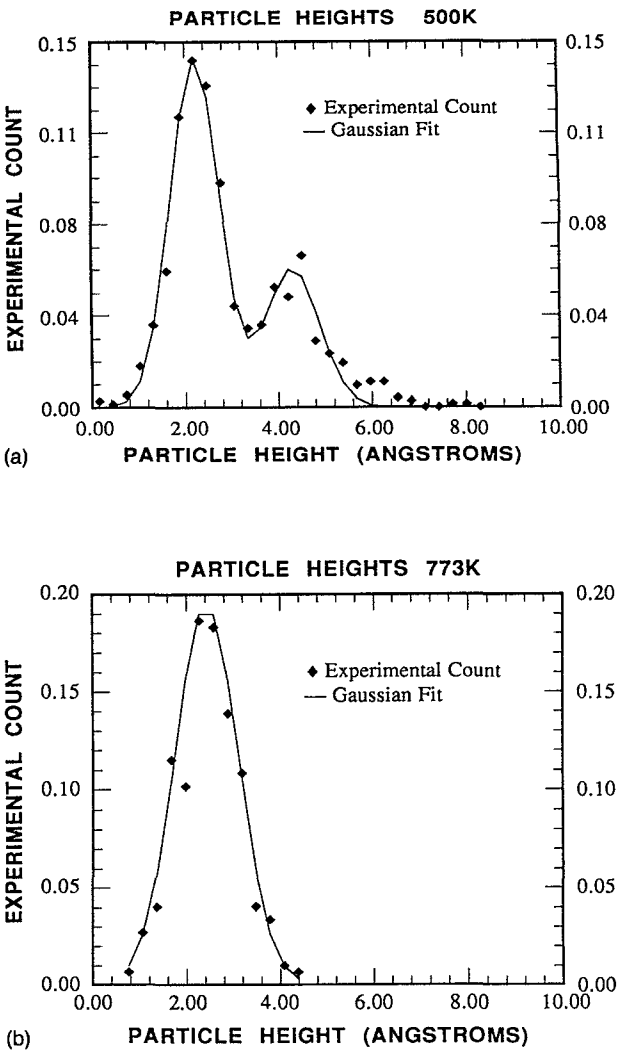

FIG. 7. Distributions of heights of carbonaceous particles observed after annealing the ethylidyne covered Pt(111) sample to (a) 500 and (b) 773 K. The distributions have been normalized to a total area under the distribution function of unity. The experimental points are indicated by ♦. The solid line indicates a fit to the experimental data by two Gaussians in the case of the 500 K results and a single Gaussian in the case of the 773 K results.

however, distributions obtained from other images at these temperatures are virtually identical to those shown. The height values have been normalized by comparison with the height of Pt steps (2.27 Å) in the same image. The actual geometric height of the adsorbate, of course, is mostly determined by electronic effects, i.e., by the local modification of the electronic structure in the presence of the adsorbate. Often this leads to apparent heights of adsorbates in STM images which are vastly different from their actual geometric height. Nevertheless the comparison of height distributions after different thermal treatments is very informative. Following the 500 K anneal, the distribution is clearly seen to be bimodal, whereas the 773 K distribution is single peaked. The solid lines in Fig. 7 are Gaussian fits to the data. The 773 K distribution is nicely fit with a single Gaussian (mean height=2.3 Å, Gaussian width=0.7 Å). The bimodal distribution obtained at 500 K can be fit with two Gaussians (mean height=2.2 Å, Gaussian width=0.7 Å; and mean height=4.3 Å, Gaussian width=0.7 Å). Since we are making observations on an atomic scale, the particle heights should, in principle, be quantized. In the present case, we assume that these curves reflect a single adsorbate species (773 K) or two different species (500 K), respectively. The width of the measured distributions may possibly reflect an inhomogeneous composition of the adparticles, but can be explained by the experimental response function.

The 773 K distribution and the first peak in the 500 K distribution are virtually identical. As we discuss more below, the small particles in the 500 K image have substantially smaller lateral dimensions than the 773 K particles.

The second peak in the 500 K distribution occurs at a particle height which is twice that of the first peak. The most straightforward interpretation would be to attribute the 773 K adparticles to monolayer islands, which are one carbon atom high, whereas at 500 K, there is a distribution of one atom high and two atom high particles. Clearly, this may be a severe simplification of the actual situation. Also, since at 500 K a substantial amount of hydrogen remains on the surface,[11,13,18] it is likely that the two atom high particles are terminated with hydrogen.

We have carried out an analysis of the number of carbon atoms per particle for the 500 K particles in the same manner as we described above. As stated earlier, this analysis assumes that all carbon on the surface is visible in the form of particles. This may be less justified at 500 K where a significant amount of hydrogen remains on the surface. Nevertheless, this analysis is informative for comparison. The adparticle density at 500 K is 2.62 times the respective density at 773 K as can be easily confirmed qualitatively by comparing Figs. 6(a) and 5(c). This analysis results in an average of 13 carbon atoms per particle. However, since we know the distribution of the two types of particles from the data in Fig. 7, we can obtain the corresponding average number of carbon atoms for each kind of particle if we assume that the two atom high particles consist of twice as many atoms as the one atom high particles. The result is that the monolayer high particles formed at 500 K have an average of ten carbon atoms per particle. The somewhat simplistic assumption that the two atom high particles have twice the number of atoms as the one atom high particles, while approximately correct, is certainly not exact since the two atom high particles in Fig. 5(c) appear to have somewhat larger in-plane dimensions compared to the one atom high particles. As we mentioned qualitatively earlier, the one atom high particles in the 500 K image are substantially smaller (in-plane dimension) than the particles in the 773 K image. This is consistent with the ten atoms per particle figure compared to the 34 atoms per particle observed for the 773 K particles. The decrease in particle density one observes in comparing the 773 K images to those obtained following annealing to 500 K also indicates significant mass transport and hence mobility of carbon containing species. At these temperatures diffusion of individual carbon atoms appears unlikely; we rather attribute this to diffusion of molecular, carbon containing, fragments or of small carbon particles.

The question of special reactivity of step edges and defects has been the focus of many studies.[21,22,25,31] The STM images in Fig. 5 and 6 allow us to decide on the activity of steps on a Pt(111) surface toward ethylene dehydrogenation by direct observation. If the step edges were to have an enhanced catalytic influence on the dehydrogenation of ethylidyne, then we would expect to see carbonaceous particles appearing first and in greater number at the step edges than on the terraces. As seen in Figs. 5 and 6, the carbonaceous particles, which are the result of dehydrogenation, appear evenly distributed over the surface and do not appear first or with any greater density at the step edges than on the terraces. From these observations, we can conclude that at least for the ethylene/ethylidyne/Pt(111) system, there does not appear to be any special reactivity toward dehydrogenation associated with the step edges. This contrasts results of an early STM investigation on ethylene/Pt(100),[40,41] where the reaction was apparently initiated at the step edges and then proceeded by later growth of the carbon covered surface areas. In the latter case, however, one has to consider the fact that this reaction is connected with a phase transition of the substrate, which might well affect or even dominate the reaction process.

FIG. 8. A 1000 Å×1000 Å image of the monolayer of graphite formed on the Pt(111) surface after annealing a saturation overlayer of ethylene to 1200 K.

Annealing the carbon covered surface to temperatures above 800 K results in the formation of graphite on the Pt surface as evidenced by the formation of the characteristic graphite rings in LEED experiments.[33,34] These findings were confirmed by experiments in our laboratory. Correspondingly with STM, we observe that the carbon clusters such as those shown in Figs. 5 and 6 form graphite islands of about 15–30 Å in diameter when the sample is annealed to 900 K. These islands exhibit the graphite structure consistent with the bulk graphite lattice spacing of 2.46 Å and are still uniformly distributed over the surface. After annealing to temperatures above 1000 K, the graphite forms larger structures on the terraces and gradually accumulates at the lower step edges forming a continuous band of domains with different rotational orientations. The formation of larger structures at the expense of the smaller ones (Ostwald ripening) and the accumulation at steps demonstrates that, above 1000 K, the C atoms become mobile on Pt(111). These effects have been discussed in detail in Ref. 4 and are illustrated here in the image shown in Fig. 8 which was obtained at room temperature after annealing at 1200 K. The honeycomb structure seen in this 1000 Å ×1000 Å image is not the actual graphite lattice, but rather a superstructure formed by the higher-order com-

FIG. 9. A 4000 Å×4000 Å image showing the effect of graphite on the Pt(111) step edge. Areas of the step edge which are decorated by graphite appear rough and irregular and areas undecorated by graphite appear clean and smooth. Note that in this large scale image, the honeycomb structure of the graphite, which is seen easily in higher resolution images, is not resolved.

mensurability of the graphite and Pt lattices at different relative rotational orientations producing various periodicity superstructures which range up to 22 Å.[4]

Coinciding with the formation of graphite on Pt following high temperature annealing of the ethylene covered surface, the influence of graphite on the Pt surface itself can be seen in the STM images. As seen in Fig. 8, areas of the Pt step edge which are decorated with graphite appear very rough and irregular. This is very different from the topography of clean Pt(111) surfaces where the step edges are straight and smooth. The smooth step edges are maintained for ethylene covered Pt (Fig. 2) or even for Pt covered with nongraphitic carbon (Figs. 2, 5, and 6), i.e., unless the Pt sample is heated above 800 K in the presence of carbon. If we use a low initial exposure of ethylene (0.15 L), we can generate step areas with and without graphite to see the effect of graphite on the step edge. Figure 9 was taken after annealing a low coverage ethylene overlayer to over 1000 K. In areas undecorated by graphite, the step edges are smooth and the Pt atoms are free to evaporate very rapidly out onto the terrace leading to the creation of the interesting, loop-like, deep hollow structures observed in the Pt step shown in Fig. 9. One can also see that decoration of the step by graphite results in roughening. The observed step roughening could occur if carbon adsorbed at the step hindered the 2D evaporation of Pt atoms from the Pt step to the terrace. There would then be rapid 2D evaporation from clean areas of the step in the neighborhood of step sites pinned by adsorbed carbon leading to step roughening. It is also possible that the roughening which we observe is due to a carbon-induced rearrangement of the Pt atoms at the step.

CONCLUSIONS

The experiments described here have resulted in several significant observations about the chemistry of the widely studied ethylene/Pt(111) system, and the STM imaging of the surface species involved. These are summarized below.

With respect to STM imaging of adsorbed molecules, we observe that ethylidyne, the stable product at 300 K resulting from the dehydrogenation of ethylene, can be imaged only by cooling the sample (to ~180 K). The temperature dependence of the ethylidyne STM images and the difference in sharpness with respect to ethylene images at the same temperature (230 K) are indicative of the disturbing effect of low frequency motions in the imaging of molecules.

With respect to the chemistry of the ethylene/Pt(111) system, the following four major points have been revealed:

(1) Since we can distinguish ethylene and ethylidyne in the STM images under reaction conditions, we have been able to watch this reaction as it occurs by reimaging an area of the surface as the reaction progresses. These experiments have revealed the unexpected result that the reaction happens in a "patchy" manner across the sample. When the reaction is only partially complete, well-defined islands of unreacted ethylene are clearly identified. Thus, at least at saturation coverage, where our experiments are

conducted, the detailed reaction mechanism is more complex than has been previously envisioned, on the basis of kinetic arguments.

(2) The dehydrogenation of ethylidyne on Pt(111) in the temperature range of 430–770 K leads to the formation of unexpectedly large three-dimensional carbonaceous particles on the surface. After annealing to 500 K, the surface is uniformly covered with carbonaceous particles which exhibit a bimodal height distribution containing roughly ten and 20 carbon atoms, respectively. The particles formed at 700 K are seen to be much more uniform, are one layer thick, and contain approximately 34 carbon atoms per particle. This somewhat surprising result means that in contrast to most of the previous literature, the carbidic carbon does not consist of individual carbon atoms or C_2 or C_3 species adsorbed on the surface, but of small agglomerates. It also may shed light on the reactivity of this carbon species, which is produced by dehydrogenation of many hydrocarbons on transition metal surfaces. The reactivity of this form of carbon on transition metals may result from the fact that much of the transition metal is still exposed in the presence of the three-dimensional carbonaceous particles.

(3) The carbonaceous particles formed in the 430–770 K range coalesce and form monolayer graphite islands when the sample is annealed at or above 800 K. Annealing above 1000 K, the initially formed 15–30 Å graphite islands grow and eventually accumulate at step edges. Graphite bonded to the Pt step edges appears to pin or even rearrange the step, resulting in a roughening of the step in areas which are decorated with carbon.

(4) The ethylene/ethylidyne conversion, the ethylidyne dehydrogenation to form carbonaceous particles, and the initial conversion of these particles to graphite islands are not affected by step defects in the Pt surface. We do not see any preferential reactivity of the Pt steps for these reactions. It is only in the later stages of graphite formation where the larger graphite islands are preferentially condensed at step edges.

These experiments show the utility of variable temperature STM for the investigation of surface chemistry. With the ability to anneal the sample at controlled temperature, and to obtain images on a short time scale after the sample temperature is changed, we were able to perform both temperature and time-dependent investigations of chemistry on the Pt surfaces. As can be seen from this study, static or time-dependent experiments involving measurements at different temperatures or following annealing to different temperatures can lead to substantial new insight into even widely studied reaction systems.

ACKNOWLEDGMENTS

One of us (T.A.L.) would like to thank the Deutscher Akademischer Austauschdienst for support in the form of a study visit fellowship. J.C.H. would like to acknowledge support of this research by the U.S. Department of Energy Grant No. DE-FG03-85ER45196.

[1] S. M. Davis and G. A. Somorjai, in *The Chemical Physics of Solid Surfaces Heterogeneous Catalysis*, edited by D. A. King and D. P. Woodruff (Elsevier, Amsterdam, 1983), Vol. 4.
[2] J. A. Horsley, in *Chemistry and Physics of Solid Surfaces VIII*, edited by R. Vanselow and R. Howe (Springer, Berlin, 1990).
[3] T. A. Land, T. Michely, R. J. Behm, J. C. Hemminger, and G. Comsa, Appl. Phys. A **53**, 414 (1991).
[4] T. A. Land, T. Michely, R. J. Behm, J. C. Hemminger, and G. Comsa, Surf. Sci. **264**, 261 (1992).
[5] J. L. Gland, F. Zaera, D. A. Fischer, R. G. Carr, and E. B. Kollin, Chem. Phys. Lett. **151**, 227 (1988).
[6] R. J. Koestner, J. Stöhr, J. L. Gland, and J. A. Horsley, Chem. Phys. Lett. **105**, 333 (1984).
[7] C. L. Pettiette-Hall, D. P. Land, R. T. McIver, and J. C. Hemminger, J. Phys. Chem. **94**, 1948 (1990).
[8] D. A. Wesner, F. P. Coenen, and H. P. Bonzel, J. Vac. Sci. Technol. A **5**, 927 (1987).
[9] L. L. Kesmodel, L. H. Dubois, and G. A. Somorjai, J. Chem. Phys. **70**, 2180 (1979).
[10] H. Steininger, H. Ibach, and S. Lehwald, Surf. Sci. **117**, 685 (1982).
[11] P. C. Stair and G. A. Somorjai, J. Chem. Phys. **66**, 2036 (1977).
[12] M. R. Albert, L. G. Sneddon, W. Eberhardt, F. Greuter, T. Gustafsson, and E. W. Plummer, Surf. Sci. **120**, 19 (1982).
[13] J. R. Creighton and J. M. White, Surf. Sci. **129**, 327 (1983).
[14] N. Freyer, G. Pirug, and H. P. Bonzel, Surf. Sci. **125**, 327 (1983).
[15] R. Yu and T. Gustafsson, Surf. Sci. **182**, L235 (1987).
[16] P. Skinner, M. W. Howard, I. A. Oxton, S. F. A. Kettle, D. B. Powell, and N. Sheppard, J. Chem., Soc. Faraday II **77**, 1203 (1981).
[17] E. A. Carter and B. E. Koel, Surf. Sci. **226**, 339 (1990).
[18] X.-L. Zhou, X.-Y. Zhu, and J. M. White, Surf. Sci. **193**, 387 (1988).
[19] M. Abon, J. Billy, and J. C. Bertolini, Surf. Sci. **171**, L387 (1986).
[20] F. L. Hutson, D. E. Ramaker, and B. E. Koel, Surf. Sci. **248**, 104 (1991).
[21] G. Somorjai, Surf. Sci. **242**, 481 (1991).
[22] F. P. Netzer and R. A. Wille, Surf. Sci. **74**, 547 (1978).
[23] K. M. Ogle, J. R. Creighton, S. Akhter, and J. M. White, Surf. Sci. **169**, 246 (1986).
[24] G. A. Somorjai, M. A. Van Hove, and B. E. Bent, J. Phys. Chem. **92**, 973 (1988).
[25] M. Salmeron and G. A. Somorjai, J. Phys. Chem. **86**, 341 (1982).
[26] R. J. Koestner, J. C. Frost, P. C. Stair, M. A. Van Hove, and G. A. Somorjai, Surf. Sci. **116**, 85 (1982).
[27] S. B. Mohsin, M. Trenary, and H. J. Robota, Chem. Phys. Lett. **154**, 511 (1989).
[28] F. Masson, C. S. Sass, O. Grizzi, and J. W. Rabalais, Surf. Sci. **221**, 299 (1989).
[29] T. A. Land, T. Michely, R. J. Behm, J. C. Hemminger, and G. Comsa (in preparation).
[30] I. V. Mitchell, W. N. Lennard, K. Griffiths, G. R. Massoumi, and J. W. Huppertz, Surf. Sci. Lett. **256**, L598 (1991).
[31] R. J. Levis, L. A. DeLouise, E. J. White, and N. Winograd, Surf. Sci. **230**, 35 (1990).
[32] B. Poelsema and G. Comsa, *Springer Tracts in Modern Physics* (Springer, Berlin, 1989), Vol. 115.
[33] B. Lang, Surf. Sci. **53**, 317 (1975).
[34] Hu Zi-pu, D. F. Ogletree, M. A. Van Hove, and G. A. Somorjai, Surf. Sci. **180**, 433 (1987).
[35] K. Besocke, Surf. Sci. **181**, 145 (1987).
[36] J. Frohn, J. F. Wolf, K. Besocke, and M. Teske, Rev. Sci. Instrum. **60**, 1200 (1989).
[37] U. Linke and B. Poelsema, J. Phys. E **18**, 26 (1985).
[38] T. Michely and G. Comsa, Surf. Sci. **256**, 217 (1991).
[39] K. H. Westmacott and M. I. Perez, Nucl. Mater. **83**, 231 (1979).
[40] W. Hösler, R. J. Behm, and E. Ritter, IBM J. Res. Develop. **30**, 403 (1986).
[41] E. Ritter, R. J. Behm, G. Pötschke, and J. Wintterlin, Surf. Sci. **181**, 403 (1987).